

# Magnetic resonance-based quantification of post-renal biopsy perirenal hematomas volumes

Piotr Białek<sup>1,A–F</sup>, Adam Dobek<sup>1,C–F</sup>, Katarzyna Szychowska<sup>2,B,C</sup>, Weronika Banasik<sup>2,B,C</sup>, Krzysztof Falenta<sup>1,C,D</sup>, Mateusz Kobierecki<sup>3,C,E,F</sup>, Ilona Kurnatowska<sup>2,B,C,E,F</sup>, Ludomir Stefańczyk<sup>1,A,C,E,F</sup>

<sup>1</sup> 1<sup>st</sup> Department of Radiology and Diagnostic Imaging, Medical University of Lodz, Poland

<sup>2</sup> Department of Internal Diseases and Transplant Nephrology, Medical University of Lodz, Poland

<sup>3</sup> Department of Diagnostic Imaging, Polish Mother's Memorial Hospital Research Institute, Łódź, Poland

A – research concept and design; B – collection and/or assembly of data; C – data analysis and interpretation;

D – writing the article; E – critical revision of the article; F – final approval of the article

Advances in Clinical and Experimental Medicine, ISSN 1899–5276 (print), ISSN 2451–2680 (online)

*Adv Clin Exp Med.* 2026;35(3):481–491

## Address for correspondence

Piotr Białek

E-mail: piotr.bialek@umed.lodz.pl

## Funding sources

This study was funded by the department's statutory research grant (grant No. 503/1-136-01/503-11-001).

## Conflict of interest

None declared

Received on February 23, 2025

Reviewed on April 25, 2025

Accepted on June 23, 2025

Published online on January 13, 2026

## Cite as

Białek P, Dobek A, Szychowska K, et al. Magnetic resonance-based quantification of post-renal biopsy perirenal hematomas volumes. *Adv Clin Exp Med.* 2026;35(3):481–491. doi:10.17219/acem/207474

## DOI

10.17219/acem/207474

## Copyright

Copyright by Author(s)

This is an article distributed under the terms of the Creative Commons Attribution 3.0 Unported (CC BY 3.0) (<https://creativecommons.org/licenses/by/3.0/>)

## Abstract

**Background.** Percutaneous renal biopsy (PRB) is the gold standard for diagnosing nephropathies but, despite being generally safe, it carries the risk of hemorrhagic complications, particularly perirenal hematomas (PHs). Ultrasound, although commonly used, tends to underestimate hematoma volumes, whereas computed tomography (CT) accurately measures volumes but poses radiation concerns and often requires contrast media. Magnetic resonance imaging (MRI), free of these risks, offers high tissue resolution but remains underutilized for PH evaluation post-PRB.

**Objectives.** To evaluate the utility of MRI-based segmentation techniques for accurately quantifying PH volumes after PRB, as a complementary imaging modality to ultrasound and CT.

**Materials and methods.** We retrospectively analyzed MRI data from 85 patients who underwent PRB between July 2020 and May 2024. MRI-derived PH volumes were measured using manual segmentation. Clinical data were extracted from patient records, and the results were compared with data from a previous CT-based study.

**Results.** Perirenal hematoma was detected in 63 patients (74.1%) with a median volume of 26.2 mL (interquartile range (IQR): 7.2–59.3 mL), slightly smaller than CT-derived volumes (median: 38 mL, IQR: 18–85 mL). Using Spearman's rank correlation coefficient (*r<sub>s</sub>*), we found that serum creatinine (Cr; *r<sub>s</sub>* = 0.299, *p* = 0.039) and systolic blood pressure (SBP; *r<sub>s</sub>* = 0.333, *p* = 0.017) correlated positively with PH volume, while hemoglobin levels showed a negative correlation (*r<sub>s</sub>* = –0.322, *p* = 0.021). Hemodialysis was associated with larger PHs (odds ratio (OR) = 4.59, 95% confidence interval (95% CI): 1.20–17.58, *p* = 0.026); however, this finding is based on a model with modest predictive performance and requires further validation.

**Conclusions.** Although its routine use may be limited, MRI could serve as a complementary tool for the detailed evaluation of PHs, offering a radiation-free and contrast media-free alternative to CT in clinical scenarios where immediate decision-making is not critical.

**Key words:** image segmentation, perirenal hematoma, kidney magnetic resonance imaging, percutaneous renal biopsy, post-biopsy bleeding complications

## Highlights

- This is the first study to use magnetic resonance imaging (MRI) to detect and quantify perirenal hematoma (PH) volumes after renal biopsy.
- MRI findings were comparable to computed tomography (CT) results, while avoiding ionizing radiation and iodinated contrast exposure.
- Serum creatinine and systolic blood pressure were significantly associated with larger PHs, whereas pre-biopsy hemoglobin showed a significant negative correlation.
- Hemodialysis status was linked to larger hematoma volumes, although the model demonstrated modest predictive performance.
- MRI may serve as a valuable complementary tool for detailed PH evaluation when immediate clinical decision-making is not required.

## Background

Percutaneous renal biopsy (PRB) is recognized as the gold standard for diagnosing a wide range of renal diseases and is generally considered a safe procedure.<sup>1–4</sup> However, it is not without risks, including complications such as macrohematuria, perirenal hematoma (PH), infection, the formation of arteriovenous fistulas, and, in rare cases, severe outcomes such as nephrectomy, the need for blood transfusions or interventional procedures, or even death.<sup>4–6</sup>

Hemorrhagic complications are the most common adverse events following PRB, PHs being the most frequently reported.<sup>4,6,7</sup> The reported incidence of PH varies widely,<sup>5</sup> ranging from as low as 1.7%<sup>8</sup> to 11% in a large meta-analysis by Poggio et al.,<sup>6</sup> and up to 86.1% in studies that employed systematic imaging with more liberal diagnostic criteria.<sup>5,7,9</sup> Most studies rely on ultrasound imaging, but there is significant heterogeneity in criteria for defining and measuring PH size in ultrasound-based research, typically measured as a PH thickness.<sup>3,6,10</sup> This variability, combined with the limitations of ultrasound in assessing the size of irregularly shaped PHs – which it often struggles to measure accurately<sup>6,11,12</sup> – may contribute to the underdiagnosis of PHs.<sup>4,12</sup>

Having researched the literature, we identified very few studies using computed tomography (CT).<sup>11,13–16</sup> Four earlier attempts, particularly in the 1980s, reported higher detection rates of PHs, with some studies noting incidences as high as 90.9%.<sup>13–16</sup> The most recent study by Chikamatsu et al.<sup>11</sup> quantified PH volume using contrast-enhanced CT and correlated it with clinical factors. Some authors argue that patients undergoing PRB should be monitored clinically rather than subjected to systematic imaging for PH, as such screening may overestimate its incidence.<sup>2,3,5</sup> This perspective likely explains the limited use of cross-sectional imaging modalities in post-PRB PH monitoring.

Given the above, the role of magnetic resonance imaging (MRI) in assessing post-PRB complications remains

underexplored. With its high soft-tissue contrast,<sup>12,17</sup> MRI has the potential to effectively evaluate PHs without the need for contrast media. However, its clinical use has been limited by availability and scan time.<sup>12,17–19</sup> We found no studies in the available literature specifically examining the use of MRI for the evaluation of PHs after PRB.

## Objectives

Consequently, this study aimed to investigate the utility of MRI for detecting post-PRB PHs. By integrating image segmentation techniques to quantify PH volume, we sought to provide precise and comprehensive insights into post-PRB PHs. We also aimed to assess the potential of MRI for these indications in comparison with CT.

## Materials and methods

This retrospective study was conducted according to the guidelines of the Declaration of Helsinki and was approved by the Bioethical Committee of the Medical University of Lodz, Poland (approval No. RNN/174/24/KE issued on July 9, 2024).

### Patient selection

All patients in this study were hospitalized in Norbert Barlicki Memorial Teaching Hospital No. 1, Medical University of Lodz, with PRBs and imaging performed in the Radiology Department. While most had native kidneys, 10 were renal transplant recipients.

Patients were eligible for inclusion if they were hospitalized in our institution, underwent PRB and had a kidney MRI performed within 36–48 h following the PRB, as, according to many authors, most PRB complications occur within the first 24 h.<sup>3,4,8,11,20–23</sup> However, a too short observation period might lead to complications being overlooked.<sup>4,23</sup> Exclusion criteria included lack of informed

consent, incomplete documentation, unavailable or poor-quality images, MRI performed outside the study protocol (i.e., not on the day following PRB), and known preexisting perirenal fluid collections. Based on these criteria, 85 subjects were enrolled.

## Renal biopsy

The PRBs were performed as a routine method for diagnosing nephropathy. Prior to the PRB assessment of vital signs, a set of laboratory tests, including coagulation parameters, was performed. Antiplatelet agents (aspirin) and direct oral anticoagulants were discontinued 5 days prior to PRB, and low-molecular-weight heparin was stopped 24 h before the procedure, in accordance with our institutional practice. Patients undergoing hemodialysis (HD) received dialysis 1 day before PRB, with heparin used during the session. In cases of thrombocytopenia, fresh frozen plasma was administered prior to the procedure. Written informed consent was obtained from all participants, who were fully informed about the procedure and cooperated satisfactorily.

Between July 2020 and May 2024, a radiologist with over 10 years of experience in ultrasound and ultrasound-guided PRB performed all PRBs under ultrasound guidance (GE Logiq 7 system; GE Healthcare, Milwaukee, USA; convex 4C probe; standard biopsy attachment). A Bard Magnum biopsy device (Bard, Covington, USA) equipped with a 16-gauge cutting needle was used for every case.

The goal was to obtain 3 tissue samples from each patient, requiring 4 needle passes in most cases. If the samples were deemed insufficient based on the immediate assessment by the performing radiologist, a 4<sup>th</sup> puncture was carried out. Importantly, no cases involved more than 4 needle passes in our practice.

Following the PRB, manual compression was applied, and patients were instructed to maintain 24 h of bed rest, including the first 4 h in the prone position. Clinical monitoring was conducted according to standard post-PRB care practices. Laboratory tests were conducted later the same day in the afternoon and were repeated 24 h after the PRB.

## MRI images acquisition and analysis

Magnetic resonance imaging was performed within 36–48 h following the PRB using a 3T scanner (Siemens Magnetom Vida; Siemens AG, Munich, Germany) equipped with an 18-channel body coil. The protocol included unenhanced sequences such as T2-weighted Half-Fourier Acquisition Single-shot Turbo spin Echo imaging with fat saturation (T2W HASTE FS) and T1-weighted (T1W) Dixon imaging (in-phase, out-of-phase, fat-only, and water-only images).

The MRI image analyses were conducted retrospectively to quantify the PH volume. Manual segmentation was performed using the Exhibeon3 DICOM viewer (Pixel

Technology, Łódź, Poland), with the two-dimensional smart brush tool applied to T1W Dixon water-only images in the coronal plane. These images were chosen for their superior ability to delineate fat tissue and blood products. Fluid collections not consistent with blood were excluded.

All segmentations, as well as their assessment and classification, were independently performed by 2 radiologists based on morphological characteristics and signal intensities consistent with the expected appearance of blood products in acute or early subacute stages on different MRI sequences.<sup>12,19</sup> In cases of disagreement, a 3<sup>rd</sup> experienced radiologist reviewed the images to ensure consensus. Representative examples are shown in Fig. 1 and Fig. 2.

## Clinical data

Clinical data, laboratory test results from the day before and the day after the PRB, as well as histological diagnoses, were retrieved from patient records. The estimated glomerular filtration rate (eGFR) was calculated using the Chronic Kidney Disease Epidemiology Collaboration (CKD-EPI) formula.<sup>24</sup> Nadler's formula<sup>25</sup> was used to calculate estimated circulating blood volume (ECBV):

$$\text{ECBV} = [\text{mL}] = 366.9 \times \text{height} [\text{m}]^3 + 32.19 \times \text{weight} [\text{kg}] + 604.1 \text{ for males}$$

and

$$\text{ECBV} = [\text{mL}] = 356.1 \times \text{height} [\text{m}]^3 + 33.08 \times \text{weight} [\text{kg}] + 183.3 \text{ for females.}$$

## Comparison to CT

To enhance our analysis and provide a comparative perspective, the data from Chikamatsu et al.<sup>11</sup> was used for evaluating CT against MRI in this context. This allowed for a comparison of the 2 imaging modalities in assessing post-PRB complications, particularly the quantification of PHs volumes. Comprehensive literature research revealed no other contemporary studies analyzing CT as a method for quantification of post-PRB PHs.

## Statistical analyses

After analyzing the baseline characteristics, the study cohort was divided into 2 subgroups: patients with PHs and those without. These groups were compared; however, only the subgroup with PHs was included in the subsequent statistical analyses. The 3<sup>rd</sup> tertile of PH volume – representing large bleeding volumes – was determined according to the methodology described by Chikamatsu et al.,<sup>11</sup> and this definition of “large PH” was used in the further evaluation.

The Shapiro–Wilk test was used to assess the normality of data distribution. Normally distributed data were presented as mean ± standard deviation (SD), while non-parametric data were reported as median and quartile

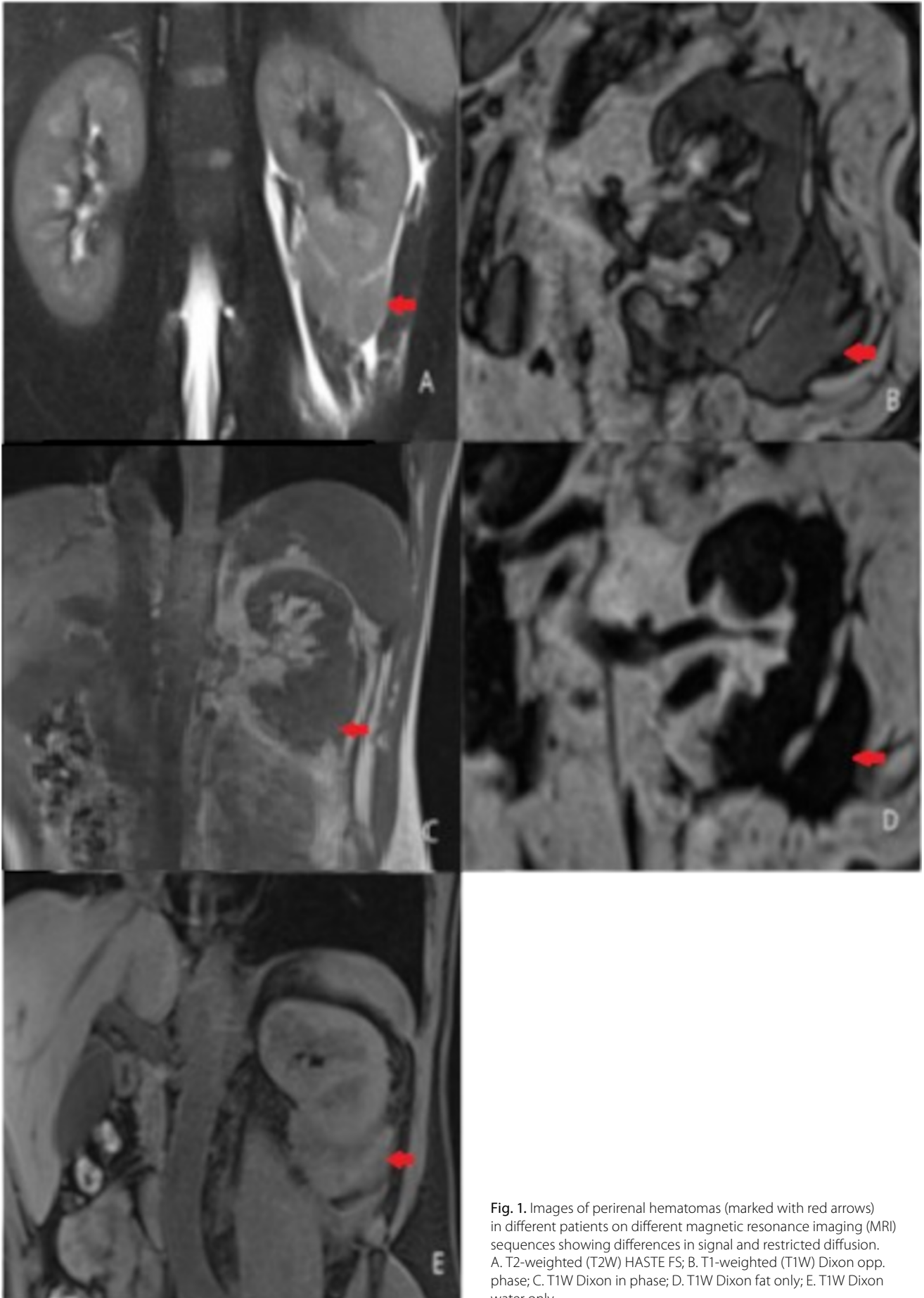


**Fig. 1.** Images of perirenal hematomas (marked with red arrows) in different patients on different magnetic resonance imaging (MRI) sequences showing differences in signal and restricted diffusion. A. T2-weighted (T2W) HASTE FS; B. T1-weighted (T1W) Dixon opp. phase; C. T1W Dixon in phase; D. T1W Dixon fat only; E. T1W Dixon water only

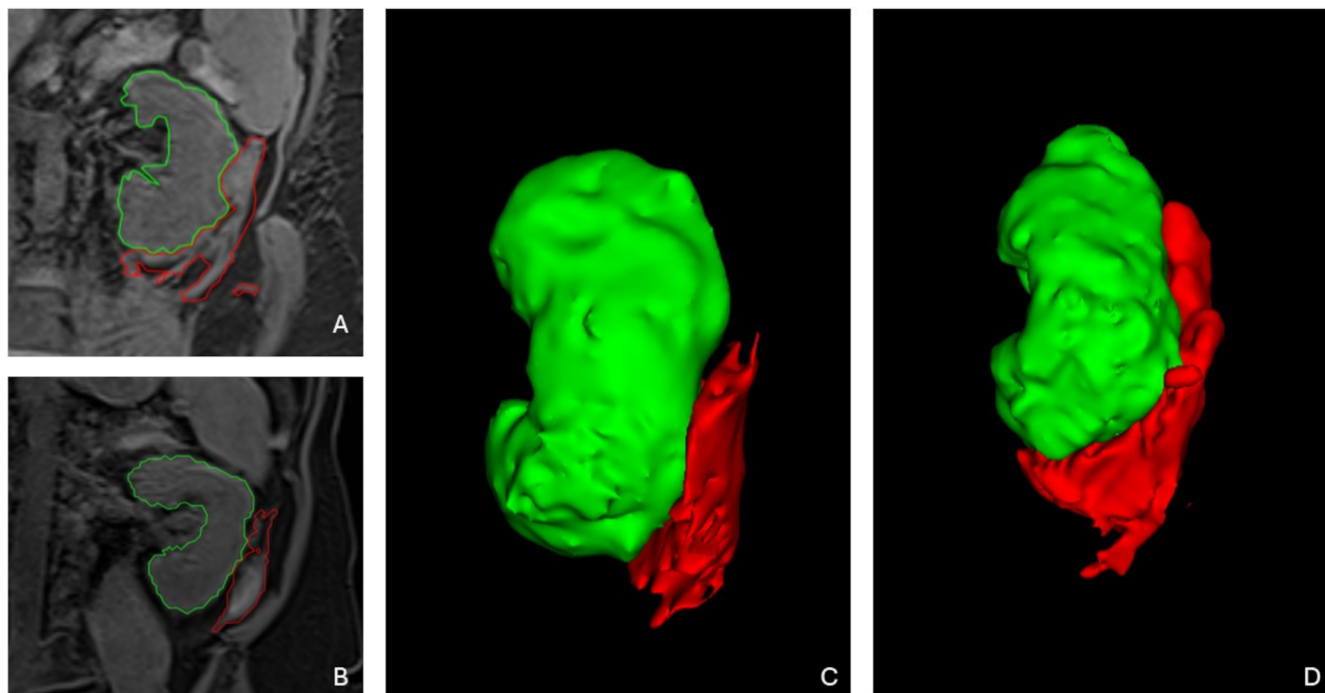


Fig. 2. Examples of perirenal hematomas in different patients. A,B. Perirenal hematomas segmentation in 2D coronal in different patients plane on T1-weighted (T1W) Dixon water only image; C,D. Volume rendered reconstructions of perirenal hematomas in these patients

red – hematoma; green – left kidney.

range (IQR). Comparisons between groups were performed using the two-tailed Student's *t*-test for parametric data and the Mann–Whitney *U* test for nonparametric data. Due to the small sample sizes in most subgroups, Fisher's exact test was employed to compare categorical variables. Kruskal–Wallis test was used to compare PH volumes in mL across different histologic types of renal diseases.

Pearson's and Spearman's correlation coefficients (*r* and *r<sub>s</sub>*, respectively) were calculated for normally and non-normally distributed data.

Multivariate logistic regression analysis was conducted to evaluate predictors associated with PH volume, specifically aiming to identify factors contributing to large PHs, defined as values in the upper tertile. The model included both continuous and categorical predictors. Continuous variables were standardized prior to model fitting. Assumptions of logistic regression were assessed: linearity between continuous predictors and the logit was tested using the Box–Tidwell test, and appropriate transformations were applied when this assumption was violated. Multicollinearity was evaluated using variance inflation factors (VIF) and tolerance values. Influential observations were identified by examining Cook's distances; cases exceeding the 4/*n* (with the sample size of 4) threshold were considered highly influential.

Statistical significance was set at *p* < 0.05, and missing data were handled by omission. All statistical analyses were performed using IBM SPSS v. 27 (IBM Corp., Armonk, USA).

## Results

The study cohort comprised 85 white adult subjects (47 males (55.3%) and 38 females (44.7%); median age 57 years; IQR: 42–64; minimum 19; maximum 82). Of these, 75 had native kidneys and 10 had renal transplants. Magnetic resonance imaging detected PH in 63 (74.1%; 56 natives, 7 transplants) and no PH in 22 (25.9%) subjects. Characteristics of the study cohort against the CT data<sup>11</sup> are presented in Table 1. Comparison between subgroups with and without PH is shown in Table 2.

The median PH volume was 26.2 mL (IQR: 7.2–59.3), *n* = 5 (8%) exceeded 100 mL; outliers reached 690 mL, and the smallest observed PH was 0.7 mL. Figure 3 and Fig. 4 depict the PH volume distribution (non-normal, *p* < 0.001).

Spearman correlation coefficients are presented in Table 3, indicating that the predictors with significant positive correlations were the pre-PRB serum creatinine level (Cr; *r<sub>s</sub>* = 0.299, *p* = 0.039) and systolic blood pressure (SBP) (*r<sub>s</sub>* = 0.333, *p* = 0.017). The only predictor with a significant negative correlation was pre-PRB hemoglobin (Hb) level (*r<sub>s</sub>* = –0.322, *p* = 0.021)

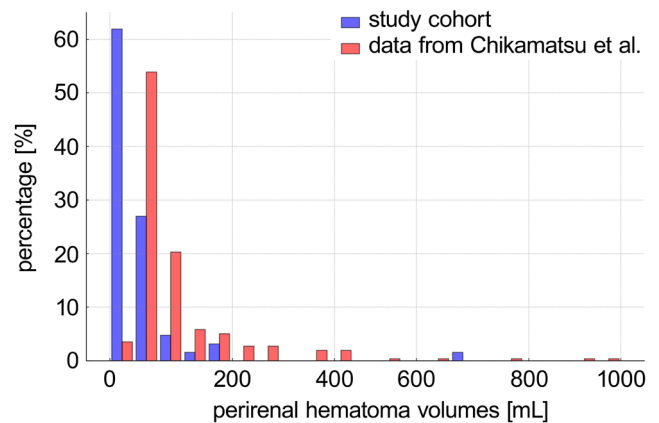
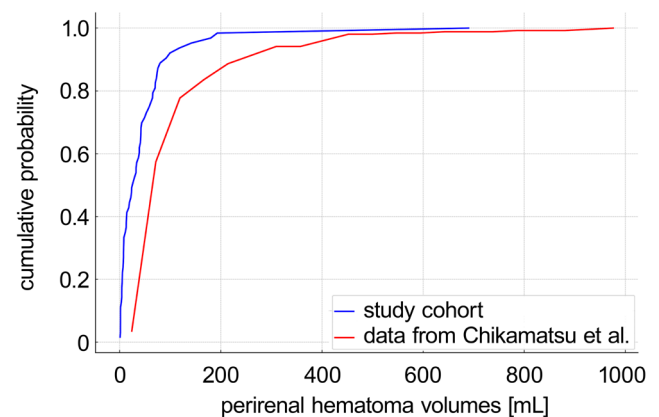
Volumes >41.8 mL (*n* = 21) constituted the 3<sup>rd</sup> tertile, whereas others (*n* = 42) were in the first 2 tertiles. Table 4 summarizes the bleeding complications observed in both the study cohort and the CT data.<sup>11</sup> Table 5 compares 3<sup>rd</sup> tertiles from this study and from Chikamatsu et al.<sup>11</sup>

No significant differences were observed across histological types with respect to the presence (H (11, 85) = 7.43,

**Table 1.** Characteristics of the study cohort and from Chikamatsu et al.<sup>11</sup>

Characteristic	Value in our study cohort	Selected values from Chikamatsu et al. <sup>11</sup>
Number of patients	85	252
Age [years]	57 (42–64)	62 ±17
Male sex, n (%)	47 (55)	153 (61)
Renal graft, n (%)	10 (12)	0 (0)
BMI [kg/m <sup>2</sup> ]	28 ±4.8	24.8 ±4.2
ECBV [mL]	4988 ±1016	3840 ±745
SBP [mm Hg]	133 ±18	139 ±25
DBP [mm Hg]	78 ±12	78 ±14
HR [bpm]	74 ±7.6	71 ±12
Creatinine [mg/dL]	1.7 (1.1–4.3)	no data
eGFR [mL/min/1.73 m <sup>2</sup> ]	38 (12–65)	44 (25–60)
HD, n (%)	18 (21)	no data
Hb before PRB [g/dL]	11.6 ±2.2	12.3 ±2.4
PLT [10 <sup>3</sup> /μL]	242 (176–299)	241 (190–300)
INR	1.01 ±0.09	no data
APTT [s]	31.5 ±3.9	30 (27–34)
Antiplatelet therapy, n (%)	2 (2)	41 (16)
Anticoagulant therapy, n (%)	34 (40)	26 (10)
Number of punctures	3 (3–3)	3 (3–4)
Histological types, n (%)		
FSGS	18 (21)	24 (10)
IgA nephropathy	11 (13)	35 (14)
Membranous nephropathy	9 (11)	11 (4)
Tubulointerstitial nephritis	8 (9)	15 (6)
Crescentic GN	8 (9)	15 (6)
ESKD	5 (6)	0 (0)
Diabetic nephropathy	4 (5)	41 (16)
Minimal change	3 (4)	15 (6)
Lupus nephritis	4 (5)	2 (1)
Pauci immune	2 (2)	0 (0)
Hypertensive nephrosclerosis	0 (0)	49 (19)
Membranoproliferative GN	1 (1)	6 (2)
Mesangial proliferative GN (non-IgA type)	0 (0)	5 (2)
Purpura nephritis	0 (0)	2 (1)
Endocapillary GN	0 (0)	1 (0)
Amyloidosis	0 (0)	1 (0)
Others	13 (15)	30 (12)

Blood pressure and laboratory results obtained before biopsy. Data are presented as mean ± standard deviation (SD), number (percentage, rounded to the nearest whole percent) or median (25<sup>th</sup>–75<sup>th</sup> percentile); BMI – body mass index; ECBV – estimated circulating blood volume; HR – heart rate; SBP – systolic blood pressure; DBP – diastolic blood pressure; eGFR – estimated glomerular filtration rate; HD – hemodialysis; Hb – hemoglobin; PRB – percutaneous renal biopsy; PT – pro-thrombin time; APTT – activated partial thromboplastin time; PLT – platelet count; FSGS – focal and segmental glomerulosclerosis; IgA – immunoglobulin A; GN – glomerulonephritis; ESKD – end-stage kidney disease.

**Fig. 3.** Histogram illustrating the perirenal hematomas (PHs) volumes distribution in the study cohort (blue) and data from Chikamatsu et al.<sup>11</sup> (red)**Fig. 4.** Distribution of perirenal hematoma (PH) volumes in study cohort (blue) and data from Chikamatsu et al.<sup>11</sup> (red) presented as cumulative distribution curves

$p = 0.764$ ) or volume in mL ( $H(10, 63) = 13.50$ ,  $p = 0.262$ ) of PH.

Due to the nonlinear relationship between eGFR and the logit (Supplementary Table 1), eGFR was modeled as a second-order polynomial (eGFR and eGFR<sup>2</sup>); alternative transformations (e.g., logarithmic, square root) were tested, but the quadratic model provided the best fit. No issues with multicollinearity were observed, as confirmed by VIF and tolerance values in Supplementary Table 2. A small number of influential cases with Cook's distance values exceeding the  $4/n$  threshold (where  $n$  denotes the sample size) were identified and temporarily excluded from analysis; however, their removal did not significantly alter the model estimates, and they were therefore retained in the final models (Supplementary Table 3).

Due to the limited size of the study cohort, we opted for 2-variable models. Estimated glomerular filtration rate was included as a core variable in all models due to its established clinical relevance as a marker of renal function.<sup>24</sup> The only multivariate logistic regression model to identify a statistically significant predictor of large PH included both eGFR and HD, with HD emerging as significant (odds ratio (OR) = 4.59, 95% confidence interval (95% CI): 1.20–17.58,

**Table 2.** Comparison between subgroups with and without PH in the study cohort

Characteristic	Value in subgroup with PH	Value in subgroup without PH	Statistical test used	Statistical test value	p-value
Number of patients (%)	63 (74)	22 (26)	–	–	–
Age [years]	58 (41–63.5)	53 ±13.5	Mann–Whitney U test	U = 683	0.924
Male sex, n (%)	33 (51)	14 (64)	Fisher’s exact test	–	0.626
Renal graft, n (%)	7 (11)	3 (14)	Fisher’s exact test	–	0.714
BMI [kg/m <sup>2</sup> ]	28.5 ±5	27 ±3.5	Student’s t-test	t(53) = 1.015	0.315
ECBV [mL]	5090 ±1085	5038 ±1049	Student’s t-test	t(47) = 0.564	0.576
SBP [mm Hg]	134.5 ±16.5	132 ±22	Student’s t-test	t(78) = 0.539	0.592
DBP [mm Hg]	78 ±11	77.5 ±13	Student’s t-test	t(78) = 0.229	0.819
HR [bpm]	72 ±8.5	75 (70–78)	Mann–Whitney U test	U = 591	0.308
Creatinine [mg/dL]	1.75 (1.1–4.5)	1.39 (1.08–4.29)	Mann–Whitney U test	U = 736	0.429
eGFR [mL/min/1.73 m <sup>2</sup> ]	37 (12–62)	58 (13–66)	Mann–Whitney U test	U = 731	0.379
HD, n (%)	15 (24)	3 (14)	Fisher’s exact test	–	0.380
Hb before PRB [g/dL]	11.8 ±2.2	11.5 ±2.2	Student’s t-test	t(77) = 0.882	0.381
PLT [10 <sup>3</sup> /μL]	244 (184–298)	247 ±101	Mann–Whitney U test	U = 768	0.755
INR	1.00 ±0.09	1.01 ±0.09	Student’s t-test	t(76) = –0.375	0.709
APTT [s]	31.6 ±4.1	31.0 ±3.5	Student’s t-test	t(76) = 0.630	0.531
Antiplatelet therapy, n (%)	2 (3)	0 (0)	Fisher’s exact test	–	>0.999
Anticoagulant therapy, n (%)	23 (37)	11 (50)	Fisher’s exact test	–	0.560
Number of punctures >3	9 (14)	7 (32)	Fisher’s exact test	–	0.112

Blood pressure and laboratory results obtained before biopsy. Data are presented as mean ± standard deviation (SD), number (percentage, rounded to the nearest whole percent) or median (25<sup>th</sup>–75<sup>th</sup> percentile); PH – perirenal hematoma; BMI – body mass index; ECBV – estimated circulating blood volume; SBP – systolic blood pressure; DBP – diastolic blood pressure; HR – heart rate; eGFR – estimated glomerular filtration rate; HD – hemodialysis; Hb – hemoglobin; PRB – percutaneous renal biopsy; PLT – platelet count; INR – International Normalized Ratio; APTT – activated partial thromboplastin time.

**Table 3.** Correlation coefficient of clinical parameters, laboratory test results and PH volume in the study cohort

Variable	Correlation coefficient	p-value
Age	–0.099	0.488
Mass	–0.010	0.943
Creatinine	0.299	0.039
eGFR	0.273	0.052
SBP	0.333	0.017
DBP	0.253	0.073
INR	0.036	0.798
APTT	–0.036	0.799
PLT	–0.008	0.952
Pre-biopsy Hb	–0.322	0.021
Needle passes	–0.215	0.129

SBP – systolic blood pressure; DBP – diastolic blood pressure; eGFR – estimated glomerular filtration rate; HD – hemodialysis; PLT – platelet count; INR – International Normalized Ratio; APTT – activated partial thromboplastin time; Hb – hemoglobin.

**Table 4.** Bleeding complications in subgroup with PHs and subjects from Chikamatsu et al.<sup>11</sup>

Bleeding complication	Value in PH subgroup	Values from Chikamatsu et al. <sup>11</sup>
PH volume [mL]	26.2 (7.2–59.3)	38 (18–85)
ECBV/PH volume (%)	0.5 (0.1–1.1)	1.1 (0.4–2.2)
Change of Hb [g/dL]	–0.05 ±0.9	–0.4 ±0.9
Macrohematuria, n (%)	12 (19)	36 (14.3)
Blood transfusion, n (%)	2 (3)	22 (8.7)
Transient hypotension, n (%)	no data	12 (4.7)
Bladder obstruction, n (%)	0 (0)	4 (1.6)
Intervention, n (%)	0 (0)	2 (0.8)

Both ECBV and PH volumes are measured in mL; therefore, in the ECBV/PH volume ratio the units cancel out, and the variable is expressed as percentage (%). Data are presented as mean ± standard deviation (SD), number (percentage, rounded to the nearest whole percent) or median (25<sup>th</sup>–75<sup>th</sup> percentile); PH – perirenal hematoma; ECBV – estimated circulating blood volume; Hb – hemoglobin; PRB – percutaneous renal biopsy.

p = 0.026). The model yielded an area under the receiver operating characteristic (ROC) curve (AUC) of 0.634 and a Nagelkerke pseudo-R<sup>2</sup> of 0.155. Further model details are provided in Table 6. Five additional 2-variable models, each including eGFR and 1 other predictor (age, sex,

SBP, anticoagulation status, or more than 3 needle passes), are presented in Supplementary Tables 4–8; none of them showed statistically significant associations.

Major clinical complications were limited to red blood cell transfusions, which occurred in 3 patients (3.5%) within

**Table 5.** Comparison of the 3<sup>rd</sup> tertile of PH volume of the study cohort and the 3<sup>rd</sup> tertile of the subjects from Chikamatsu et al.<sup>11</sup>

Characteristic	Value in the 3 <sup>rd</sup> tertile of subgroup with PH	Selected values in the 3 <sup>rd</sup> tertile from Chikamatsu et al. <sup>11</sup>
Number of patients	21	84
Age [years]	52 ±16.5	61 ±17
Male sex, n (%)	12 (57)	48 (57)
Renal graft, n (%)	1 (5)	0 (0)
BMI [kg/m <sup>2</sup> ]	28.4 ±6.4	25.4 ±4.1
SBP [mm Hg]	139 ±13	140 ±29
DBP [mm Hg]	81 ±11	80 ±13
HR [bpm]	71 ±8	71 ±13
Creatinine [mg/dL]	3.4 (1.25–6.7)	no data
eGFR [mL/min/1.73 m <sup>2</sup> ]	21 (8–61)	38 (25–62)
HD, n (%)	8 (38)	no data
Hb before PRB [g/dL]	11.3 ±1.8	12.4 ±2.6
PLT [10 <sup>3</sup> /μL]	235 ±86	242 (179–303)
INR	0.98 ±0.09	no data
APTT [s]	30.7 ±3.4	no data
Antiplatelet therapy, n (%)	0 (0)	17 (20)
Anticoagulant therapy, n (%)	10 (48)	11 (13)
Number of punctures	3.0 (3.0–3.0)	3.0 (3.0–4.0)
PH volume [mL]	72.6 (61.2–99.3)	126 (85–203)
Change of Hb [g/dL]	–0.1 ±1.0	–0.9 ±1.0
Macrohematuria, n (%)	4 (19)	12 (14)
Blood transfusion, n (%)	1 (5)	8 (10)

Vital signs and laboratory results obtained before biopsy. Data are presented as mean ± standard deviation (SD), number (percentage, rounded to the nearest whole percent) or median (25<sup>th</sup>–75<sup>th</sup> percentile); PH – perirenal hematoma; BMI – body mass index; SBP – systolic blood pressure; DBP – diastolic blood pressure; HR – heart rate; eGFR – estimated glomerular filtration rate; HD – hemodialysis; Hb – hemoglobin; PRB – percutaneous renal biopsy; PLT – platelet count; INR – International Normalized Ratio; APTT – activated partial thromboplastin time.

the 1<sup>st</sup> 24 h after PRB: 2 patients (3.2%) in the subgroup with PH and 1 patient (0.5%) in the subgroup without PH. We also observed gross hematuria in 12 subjects. No other major complications were noted. Outlier cases generally showed markedly elevated Cr and reduced eGFR. The largest PH (690 mL) was observed in a 70-year-old male with membranous nephropathy and kidney failure

(Cr 5.1 mg/dL, eGFR 12 mL/min/1.73 m<sup>2</sup>, pre-PRB Hb 8.5 g/dL decreasing to 7.3 g/dL). No additional risk factors were identified in this case, which was managed with red blood cell transfusion. However, another subject transfused within 24 h had a comparatively small PH volume of 18 mL.

## Discussion

Our study revealed a PH prevalence of 74.1%, aligning with findings from the past CT-based studies<sup>13–16</sup> and exceeding the rates reported in ultrasound-based studies, such as the 11% observed in a large meta-analysis by Poggio et al.<sup>6</sup> Remarkably, we found no significant differences in demographic or clinical data between subjects with and without PH. We hypothesize that this may stem from the superior sensitivity of MRI in detecting very small PHs (e.g., 0.7 mL).

Our findings showed notable similarities to those of Chikamatsu et al.,<sup>11</sup> particularly regarding PH volumes, though our results indicated slightly smaller values. Specifically, the median PH volume in our study was 26.2 mL (IQR: 7.2–59.3), compared to 38 mL (IQR: 18–85) in their analysis. It is plausible that the slightly smaller PH volumes observed in our study may be attributed not only to different imaging modality of PH detection, but also to the absence of cases involving more than 4 punctures, a factor identified by Chikamatsu et al. as a significant predictor of larger PH volumes.<sup>11</sup> Notably, our cohort included only subjects with 3 or 4 punctures, and none exceeding 4. Consequently, our multivariate logistic regression analysis found no significant association between needle passes and PH volume ( $p = 0.161$ ), which is consistent with those of some other studies.<sup>5,20,26,27</sup> Additionally, we observed less pronounced changes in Hb levels following PRB ( $0.05 \pm 0.9$  vs  $0.4 \pm 0.9$ ) and fewer complications, including lower blood transfusion rates and no need for interventions. These smaller changes in Hb levels may partly reflect the ECBV in our cohort, potentially linked to demographic differences between the study populations.

We demonstrated a positive correlation between Cr and PH ( $r_s = 0.299$ ,  $p = 0.039$ ), consistent with findings reported by other authors.<sup>2,5,23,28,29</sup> A positive correlation was also observed between SBP and PH ( $r_s = 0.333$ ,  $p = 0.017$ ), also in line with prior literature.<sup>26,28,29</sup> Conversely,

**Table 6.** Multivariate logistic regression model including eGFR and HD as predictors of large post-biopsy PHs

Variable	B	B lower 95% CI	B upper 95% CI	SE	z	Wald	OR	OR lower 95% CI	OR upper 95% CI	p-value
Intercept	–1.084	–1.775	–0.393	0.353	–3.075	6.406	0.338	0.169	0.675	0.002
eGFR	0.868	–0.637	2.373	0.768	1.131	9.458	2.382	0.529	10.724	0.258
HD	1.524	0.181	2.867	0.685	2.224	1.278	4.590	1.198	17.582	0.026

AUC = 0.634; Nagelkerke pseudo- $R^2 = 0.155$ ; AIC = 75.276; BIC = 81.559. B – regression coefficient; SE – standard error; z – z-statistic; Wald – Wald  $\chi^2$  statistic; OR – odds ratio; 95% CI – 95% confidence interval; eGFR – estimated glomerular filtration rate; HD – hemodialysis AUC – area under the curve; AIC – Akaike Information Criterion; BIC – Bayesian Information Criterion.

a significant negative correlation was found between Hb and PH ( $r_s = -0.322$ ,  $p = 0.021$ ). This observation is supported by the findings of both Lim et al. and Palsson et al., who independently identified low Hb levels prior to PRB as a significant predictor of major bleeding complications and the need for transfusion following renal biopsy.<sup>30,31</sup>

Furthermore, our analysis underscored that HD treatment may be associated with an elevated risk of larger PH volume (OR = 4.59, 95% CI: 1.20–17.58,  $p = 0.026$ ). However, the relatively small number of HD patients ( $n = 18$ ) may have limited both the precision of the estimate and the overall discriminatory ability of the model, which demonstrated a modest AUC of 0.634 and very low explanatory power, as indicated by a Nagelkerke pseudo- $R^2$  of 0.155. This value of the Nagelkerke pseudo- $R^2$  indicates that the model explained approx. 15.5% of the variance in PH volume, suggesting that additional relevant variables likely contribute to the outcome and were not captured in the current analysis. Nevertheless, the observed association aligns with the general understanding of impaired renal function as a predictor of post-PRB bleeding complications,<sup>5,6,9,28</sup> yet studies explicitly examining the direct link between HD and PH risk remain limited. For instance, Simard-Meilleur et al. also identified HD as a significant risk factor of PH, while, similarly to our findings, they did not find eGFR to be an independent predictor.<sup>20</sup> In our study, a potential contributing factor in this context may be the use of heparin during the HD session performed 1 day prior to the PRB. Altogether, these findings highlight the need for further research to clarify the role of HD in post-PRB hemorrhagic risk, particularly in larger patient cohorts to improve the robustness and generalizability of the findings.

Similar to CT-based study,<sup>11</sup> we observed no significant differences in hemorrhage volumes across histologic types. This finding contrasts with some reports,<sup>26,27</sup> yet aligns with others,<sup>31</sup> reflecting the variability present in the literature. Several demographic and clinical predictors have been proposed by different authors, including age – either younger<sup>1,27,32</sup> or older<sup>2,5</sup> – and female gender.<sup>27,32</sup> However, the significance of these factors has varied across studies, likely due to differences in methodology, patient populations and clinical settings. In our analysis, none of these variables reached statistical significance.

Despite its advantages, MRI has several limitations as an imaging modality. It is not only less widely available than CT,<sup>19,33</sup> but its use is also restricted in patients with certain metallic implants or devices, such as pacemakers.<sup>12</sup> Additionally, MRI requires significantly more time for image acquisition.<sup>12,17–19</sup> In our study, the average MRI scan duration was approx. 19 min – much longer than a CT scan, which takes only seconds for a single phase.<sup>12</sup> While CT in the context of acute renal hemorrhage should be multiphasic,<sup>12,34</sup> it is still much faster than MRI, which is also more prone to motion artifacts due to the extended acquisition time. In cases of active bleeding MRI can delay patient management,<sup>12</sup> which is critical when urgent

interventional treatment may be required.<sup>34</sup> Another significant limitation of MRI in this context is the variable appearance of blood products depending on their age, potentially leading to ambiguous findings,<sup>12,19</sup> which require time and expertise to interpret accurately.

Many authors<sup>2,3,5,6</sup> emphasize that patients post-PRB should be primarily monitored through clinical observation, including vital signs, presence of hematuria and laboratory parameters such as Hb levels. Although clinical observation remains the cornerstone of post-PRB monitoring, several studies have demonstrated that it may fail to detect subclinical PHs, which can be identified only through imaging.<sup>16,21,23</sup> The stability of the hemodynamic status of the patient is a key determinant in selecting the appropriate imaging modality and further management.<sup>12,35</sup> Ultrasound should serve as the first-line imaging modality for the rapid initial detection of potential hemorrhage,<sup>34</sup> although it has limited sensitivity for identifying hemorrhage in the retroperitoneal space.<sup>12,34</sup> If active bleeding is suspected, contrast-enhanced CT should be employed as the imaging modality of choice<sup>12</sup> to confirm the diagnosis and guide further interventional planning.<sup>12,34</sup>

From this perspective, although its routine use may be limited,<sup>34</sup> MRI may serve as a valuable complementary tool for comprehensive assessment in appropriate clinical scenarios. Magnetic resonance imaging may be better suited for detailed evaluation in subacute circumstances, particularly when prior imaging yields inconclusive results,<sup>12,19</sup> for distinguishing between acute and chronic blood deposits<sup>12,19</sup> or for detection of potential underlying hemorrhage causes such as neoplasms.<sup>12</sup> In contrast, CT remains the preferred modality when rapid decision-making is essential.<sup>12,34,35</sup> Based on these considerations, a stepwise diagnostic strategy can be proposed that prioritizes modality selection according to clinical urgency, stability and information yield. As outlined in Table 7, this practical algorithm begins with clinical observation, followed by ultrasound as the first-line imaging tool. Computed tomography is employed when active bleeding is suspected and rapid interventional planning is required. Magnetic resonance imaging is reserved for stable patients requiring detailed characterization of PHs or when other modalities provide inconclusive results, particularly where avoiding contrast media or radiation is preferred.

## Limitations of the study

Several limitations of our study should be noted. It was conducted retrospectively, and the cohort was relatively small and heterogeneous, encompassing both native kidneys and renal grafts. Importantly, there was no direct comparison of imaging methods; instead, our findings were compared to literature data from the only similar study,<sup>11</sup> which inherently limits the generalizability of our conclusions. This comparison is further complicated by cohort heterogeneity and demographic differences,

**Table 7.** Proposed sequential diagnostic algorithm for the assessment of PHs following PRB

Step	Indications and advantages	Limitations
Step 1: Clinical observation	<ul style="list-style-type: none"> <li>Monitor vital signs, hematuria and laboratory findings (e.g., hemoglobin levels) after PRB<sup>2,3,5,6</sup></li> <li>Critical in determining the need for and type of imaging<sup>12,35</sup></li> </ul>	<ul style="list-style-type: none"> <li>May miss subclinical bleeding<sup>16,21,23</sup></li> <li>No imaging data provided</li> </ul>
Step 2: Ultrasound	<ul style="list-style-type: none"> <li>First-line imaging for rapid detection of hemorrhage<sup>34</sup></li> <li>Widely available, bedside-capable</li> <li>Radiation-free</li> </ul>	<ul style="list-style-type: none"> <li>Limited sensitivity in the retroperitoneum; may fail to detect some PHs<sup>12,34</sup></li> <li>Cannot reliably determine whether bleeding is active<sup>12</sup></li> <li>Not reliable for accurate volume estimation or irregular shapes<sup>6,11,12</sup></li> </ul>
Step 3: CT	<ul style="list-style-type: none"> <li>Widely available<sup>19,33</sup></li> <li>Indicated when active bleeding is suspected<sup>12</sup></li> <li>High diagnostic value<sup>12</sup></li> <li>Suitable for interventional planning<sup>12</sup></li> <li>Shorter scan time than MRI<sup>18</sup></li> </ul>	<ul style="list-style-type: none"> <li>Ionizing radiation</li> <li>Not always feasible in patients with contrast allergy or poor renal function</li> <li>Worse soft tissue contrast than MRI</li> </ul>
Adjunct: MRI	<ul style="list-style-type: none"> <li>Offers excellent soft tissue contrast even without contrast media<sup>12,17</sup></li> <li>Radiation-free</li> <li>Precise PH volume quantification</li> <li>Useful for characterizing PH age or detecting potential underlying causes<sup>12,19</sup></li> </ul>	<ul style="list-style-type: none"> <li>Limited availability<sup>19,33</sup></li> <li>Sometimes difficult interpretation<sup>12,19</sup></li> <li>Not recommended in acute bleeding<sup>12</sup></li> <li>Longer scan time, motion artifacts<sup>18</sup></li> <li>Contraindicated with some metallic implants or devices<sup>12</sup></li> </ul>

PRB – percutaneous renal biopsy; Hb – hemoglobin; PH – perirenal hematoma; CT – computed tomography; MRI – magnetic resonance imaging.

affecting generalizability. The limited existing literature on cross-sectional imaging for the detection of PHs after PRB underscores the exploratory nature of our research, which we consider a pilot study. Additionally, interobserver variability in manual segmentation was not formally assessed, though all segmentations were reviewed and agreed upon by experienced radiologists to ensure reliability.

## Conclusions

Our study highlights the potential of MRI in the assessment of PHs following PRB, offering precise volume quantification comparable to CT while avoiding the risks of ionizing radiation and contrast media. Although its routine use may be limited, MRI can serve as a complementary tool for detailed evaluation of PHs in clinical scenarios when immediate decision-making is not critical.

## Supplementary data

The supplementary materials are available at <https://doi.org/10.5281/zenodo.15600431>. The package contains the following files:

Supplementary Table 1. Assessment of linearity of continuous predictors with the logit using the Box–Tidwell test.

Supplementary Table 2. Assessment of multicollinearity using tolerance and VIF in logistic regression models.

Supplementary Table 3 Assessment of influential observations in logistic regression models using Cook's distance.

Supplementary Table 4. Multivariate logistic regression model including eGFR and age as predictors of large post-biopsy PHs.

Supplementary Table 5. Multivariate logistic regression model including eGFR and gender as predictors of large post-biopsy PHs.

Supplementary Table 6. Multivariate logistic regression model including eGFR and SBP as predictors of large post-biopsy PHs.

Supplementary Table 7. Multivariate logistic regression model including eGFR and anticoagulation as predictors of large post-biopsy PHs.

Supplementary Table 8. Multivariate logistic regression model including eGFR and number of needle passes as predictors of large post-biopsy PHs.

## Data Availability Statement

The participants of this study did not give written consent for their data to be shared publicly, so due to the sensitive nature of the research, the supporting data are not available.

## Consent for publication

Not applicable.

## Use of AI and AI-assisted technology

Not applicable.

## ORCID iDs

Piotr Białek  <https://orcid.org/0009-0006-8816-7201>

Adam Dobek  <https://orcid.org/0000-0002-9675-1938>

Krzysztof Falenta  <https://orcid.org/0009-0009-1860-9870>

Mateusz Kobierecki  <https://orcid.org/0000-0003-2559-5840>

Ilona Kurnatowska  <https://orcid.org/0000-0003-3448-0682>

Ludomir Stefańczyk  <https://orcid.org/0000-0002-0474-7430>

## References

- Montes D, Beamish C, Waheed S, Osman F, Maursetter L. What happens after the kidney biopsy? The findings nephrologists should know. *BMC Nephrol.* 2022;23(1):265. doi:10.1186/s12882-022-02881-w
- Tøndel C, Vikse BE, Bostad L, Svarstad E. Safety and complications of percutaneous kidney biopsies in 715 children and 8573 adults in Norway 1988–2010. *Clin J Am Soc Nephrol.* 2012;7(10):1591–1597. doi:10.2215/CJN.02150212
- Hogan JJ, Mocanu M, Berns JS. The native kidney biopsy: Update and evidence for best practice. *Clin J Am Soc Nephrol.* 2016;11(2):354–362. doi:10.2215/CJN.05750515
- Schnuelle P. Renal biopsy for diagnosis in kidney disease: Indication, technique, and safety. *J Clin Med.* 2023;12(19):6424. doi:10.3390/jcm12196424
- Corapi KM, Chen JLT, Balk EM, Gordon CE. Bleeding complications of native kidney biopsy: A systematic review and meta-analysis. *Am J Kidney Dis.* 2012;60(1):62–73. doi:10.1053/j.ajkd.2012.02.330
- Poggio ED, McClelland RL, Blank KN, et al. Systematic review and meta-analysis of native kidney biopsy complications. *Clin J Am Soc Nephrol.* 2020;15(11):1595–1602. doi:10.2215/CJN.04710420
- Tanaka K, Kitagawa M, Onishi A, et al. Arterial stiffness is an independent risk factor for anemia after percutaneous native kidney biopsy. *Kidney Blood Press Res.* 2017;42(2):284–293. doi:10.1159/000477453
- Prasad N, Kumar S, Manjunath R, et al. Real-time ultrasound-guided percutaneous renal biopsy with needle guide by nephrologists decreases post-biopsy complications. *Clin Kidney J.* 2015;8(2):151–156. doi:10.1093/ckj/sfv012
- Ishikawa E, Nomura S, Hamaguchi T, et al. Ultrasonography as a predictor of overt bleeding after renal biopsy. *Clin Exp Nephrol.* 2009;13(4):325–331. doi:10.1007/s10157-009-0165-7
- Waldo B, Korbet SM, Freimanis MG, Lewis EJ. The value of post-biopsy ultrasound in predicting complications after percutaneous renal biopsy of native kidneys. *Nephrol Dial Transplant.* 2009;24(8):2433–2439. doi:10.1093/ndt/gfp073
- Chikamatsu Y, Matsuda K, Takeuchi Y, et al. Quantification of bleeding volume using computed tomography and clinical complications after percutaneous renal biopsy. *Clin Kidney J.* 2017;10(1):9–15. doi:10.1093/ckj/sfw131
- Verma N, Steigner ML, Aghayev A, et al. ACR Appropriateness Criteria® Suspected Retroperitoneal Bleed. *J Am Coll Radiol.* 2021;18(11 Suppl):S482–S487. doi:10.1016/j.jacr.2021.09.003
- Ralls PW, Barakos JA, Kaptein EM, et al. Renal biopsy-related hemorrhage: Frequency and comparison of CT and sonography. *J Comput Assist Tomogr.* 1987;11(6):1031–1034. doi:10.1097/00004728-198711000-00021
- Ginsburg JC, Fransman SL, Singer MA, Cohan M, Morrin PAF. Use of computerized tomography to evaluate bleeding after renal biopsy. *Nephron.* 1980;26(5):240–243. doi:10.1159/000181992
- Alter AJ, Zimmerman S, Kirachaiwanich C. Computerized tomographic assessment of retroperitoneal hemorrhage after percutaneous renal biopsy. *Arch Intern Med.* 1980;140(10):1323–1326. PMID:7425767.
- Rosenbaum R, Hoffsten PE, Stanley RJ, Klahr S. Use of computerized tomography to diagnose complications of percutaneous renal biopsy. *Kidney Int.* 1978;14(1):87–92. doi:10.1038/ki.1978.93
- Kobi M, Flusberg M, Chernyak V. MR imaging of acute abdomen and pelvis. *Curr Radiol Rep.* 2016;4(6):33. doi:10.1007/s40134-016-0160-1
- Edelstein WA, Mahesh M, Carrino JA. MRI: Time is dose and money and versatility. *J Am Coll Radiol.* 2010;7(8):650–652. doi:10.1016/j.jacr.2010.05.002
- Ku J, Jeon Y, Kim M, Lee N, Park Y. Is there a role for magnetic resonance imaging in renal trauma? *Int J Urol.* 2001;8(6):261–267. doi:10.1046/j.1442-2042.2001.00297.x
- Simard-Meilleur MC, Troyanov S, Roy L, Dalaire E, Brachemi S. Risk factors and timing of native kidney biopsy complications. *Nephron Extra.* 2014;4(1):42–49. doi:10.1159/000360087
- Korbet SM, Volpini KC, Whittier WL. Percutaneous renal biopsy of native kidneys: A single-center experience of 1,055 biopsies. *Am J Nephrol.* 2014;39(2):153–162. doi:10.1159/000358334
- Stratta P, Canavese C, Marengo M, et al. Risk management of renal biopsy: 1387 cases over 30 years in a single centre. *Eur J Clin Invest.* 2007;37(12):954–963. doi:10.1111/j.1365-2362.2007.01885.x
- Whittier WL, Korbet SM. Timing of complications in percutaneous renal biopsy. *J Am Soc Nephrol.* 2004;15(1):142–147. doi:10.1097/01.ASN.0000102472.37947.14
- Levey AS, Stevens LA, Schmid CH, et al. A new equation to estimate glomerular filtration rate. *Ann Intern Med.* 2009;150(9):604–612. doi:10.7326/0003-4819-150-9-200905050-00006
- Nadler SB, Hidalgo JH, Bloch T. Prediction of blood volume in normal human adults. *Surgery.* 1962;51(2):224–232. PMID:21936146.
- Eiro M, Katoh T, Watanabe T. Risk factors for bleeding complications in percutaneous renal biopsy. *Clin Exp Nephrol.* 2005;9(1):40–45. doi:10.1007/s10157-004-0326-7
- Peters B, Stegmayr B, Andersson Y, Hadimeri H, Mölne J. Increased risk of renal biopsy complications in patients with IgA-nephritis. *Clin Exp Nephrol.* 2015;19(6):1135–1141. doi:10.1007/s10157-015-1121-3
- Shidham GB, Siddiqi N, Beres JA, et al. Clinical risk factors associated with bleeding after native kidney biopsy. *Nephrology.* 2005;10(3):305–310. doi:10.1111/j.1440-1797.2005.00394.x
- Roccatello D, Sciascia S, Rossi D, et al. Outpatient percutaneous native renal biopsy: Safety profile in a large monocentric cohort. *BMJ Open.* 2017;7(6):e015243. doi:10.1136/bmjopen-2016-015243
- Lim CC, Tan RY, Choo JC, et al. Estimation of risk for major bleeding in native kidney biopsies in patients with multiple risk factors. *Int Urol Nephrol.* 2022;54(2):343–348. doi:10.1007/s11255-021-02874-y
- Palsson R, Short SAP, Kibbelaar ZA, et al. Bleeding complications after percutaneous native kidney biopsy: Results from the Boston Kidney Biopsy Cohort. *Kidney Int Rep.* 2020;5(4):511–518. doi:10.1016/j.ekir.2020.01.012
- Peters B, Nasic S, Segelmark M. Clinical parameters predicting complications in native kidney biopsies. *Clin Kidney J.* 2020;13(4):654–659. doi:10.1093/ckj/sfz132
- Ginde AA, Foianini A, Renner DM, Valley M, Camargo, Jr CA. Availability and quality of computed tomography and magnetic resonance imaging equipment in U.S. emergency departments. *Acad Emerg Med.* 2008;15(8):780–783. doi:10.1111/j.1553-2712.2008.00192.x
- Dayal M, Gamanagatti S, Kumar A. Imaging in renal trauma. *World J Radiol.* 2013;5(8):275. doi:10.4329/wjrv.v5.i8.275
- Coccolini F, Moore EE, Kluger Y, et al. Kidney and uro-trauma: WSES-AAST guidelines. *World J Emerg Surg.* 2019;14(1):54. doi:10.1186/s13017-019-0274-x